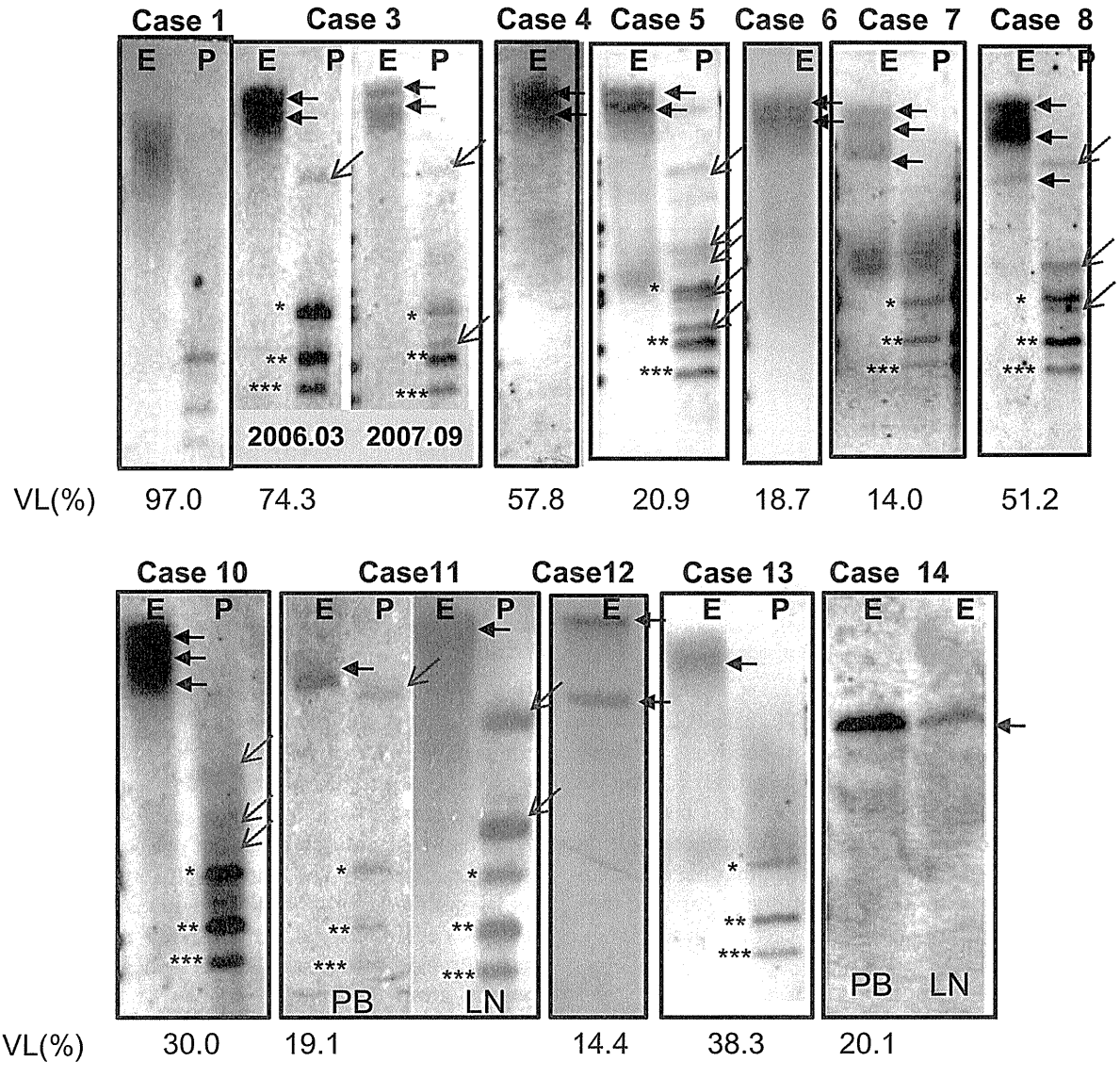

Figure 2 Representative band patterns by SBH analysis in high VL carriers with dense smears, aberrant-bands with/without faint sharp band(s). E & P; EcoR1 and Pst-1 digestion, *, **, ***; internal bands after Pst-1 digestion, ; clonal band(s), PB; peripheral blood, LN; lymph node. Case 1: Typical dense smeared band, case 3: probably two bands within dense smeared bands in March, 2006, and clear multi-bands in September, 2007. Cases 4, 5, 6, 7, 8, and 10; two or more vague clonal band(s). Case 11; different band sizes between peripheral blood (PB) and lymph nodes (LN), Cases 12 and 13; two clonal bands and an atypical broad band, Case 14; the same band size for LN and blood.

strongyloidosis and HTLV-1 have been reported to harbor a higher VL of around 50% with a high incidence (39%) of clonality [16,17]. The relation between VL and clonality is controversial [11,12] because the decision regarding clonality depends on the sensitivity of the method.

Taken together, our study supports the idea that extremely high VL mainly results from polyclonal expansion of HTLV-1 infected cells at the sensitive level of SBH.

In samples from patients with lymphoma-type ATL without ATL cells, a clonal band(s) was demonstrated in 4 of the 8 patients. Band size between blood and lymph nodes was the same in two of the 4 cases, but no circulating ATL was found. Other aberrant bands, as summarized in Additional file 1, were also observed. Such a band profile in ATL (lymphoma-type) appears to be looks a relic of a symptomatic carriers' past, indicating that high VL with aberrant bands could become a biomarker to

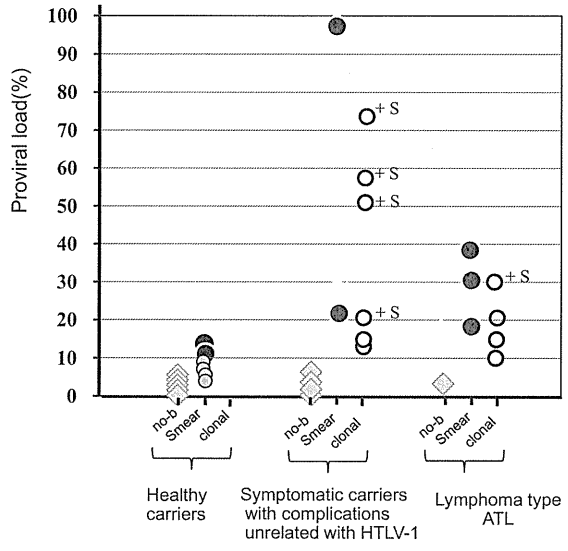

Figure 3 A comparison between the level of VL and SBH status among healthy asymptomatic carriers, symptomatic carriers with complications unrelated to HTLV-1, and patients with lymphoma type ATL. Gray diamond; no-band, gray circle; vague to faint smears, solid circle; dense smears, open circle; clonal band, +S: mixture band of dense smears and conal bands.

predict the development of ATL. Indeed, cases 3 and 5 developed smoldering ATL after 4 years and acute ATL after 3 years, respectively. A conceptual scheme is presented in Figure 5, which shows the biological significance of the fluctuation in a high VL with either dense smears or oligoclonal bands durig multi-step leukomogenesis as a stone corner of dense smear emergence.

Conclusion

Focusing on not only discrete clonal band(s), but also aberrant smears, it is noteworthy that the emergence of dense smears equivalent to polyclonal expansion of infected cells mainly contributed to a high level VL. However, it is reasonable that a high VL does not consist of only polyclonally expanded infected cells, but included abundant small clones in the cell population, because of sensitivity in SBH. SBH for HTLV-1 could evaluate or monitor the clinical clonal status of HTLV-1-infected cells. Clinically, the distinctive profile of high VL and aberrant band status is expected to monitor or predict some events caused by HTLV-1.

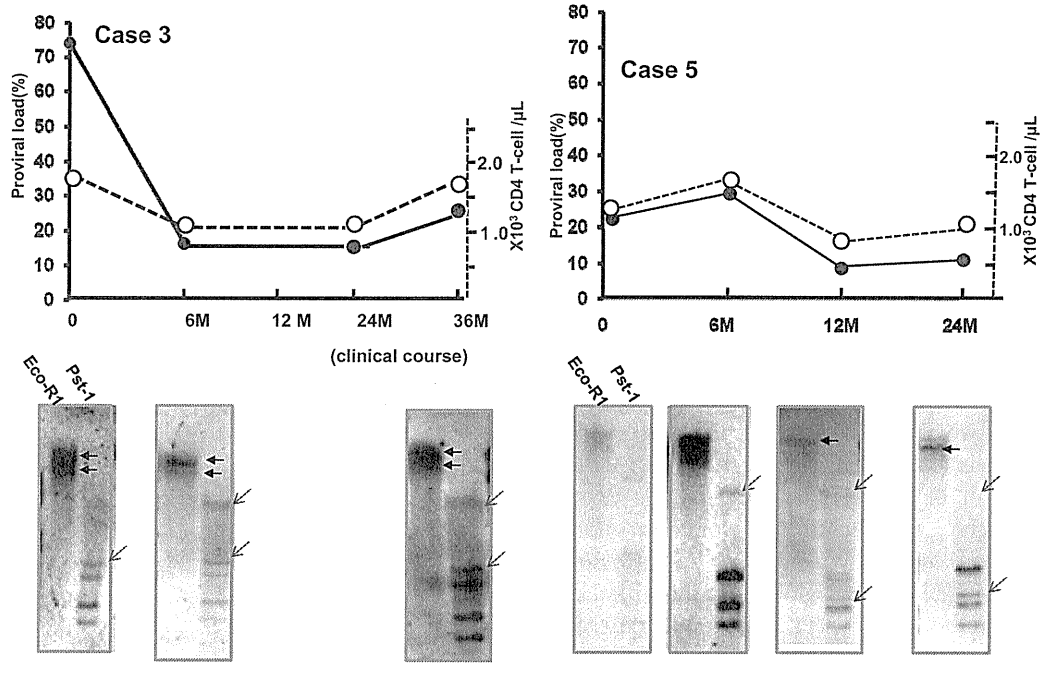

Figure 4 Upper panel shows the sequential measurement of VL (%; solid line) and CD4T-cell number/μL (broken line) in symptomatic cases 3 and 5. Lower panel shows SBH status at the same time as VL assays. In case 3, the first SBH gave dense smears (black arrow, Eco-R1 digestion) and an indeterminate clonal band (red arrow, Pst1 digestion), and then dense smears disappeared followed by clear visualization of a clonal band. In case 5, when dense smears emerged, the VL was the highest, and after disappearance, the clonal band and level of VL stably persisted.

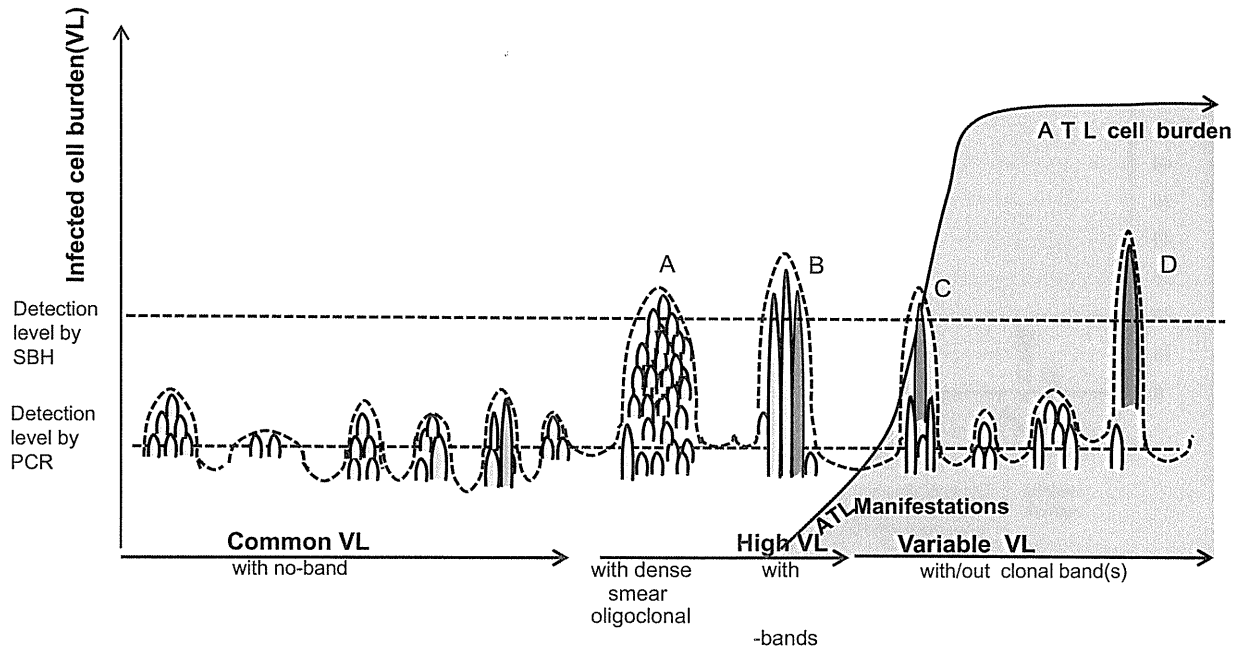

Figure 5 Conceptual scheme of the fluctuations in the total proviral load (VL) in peripheral blood with no circulating abnormal cells during multi-step leukemogenesis. VL is low in the early phase of the latent period, during which infected cells consist of clones with a small population. At some time point, some clones may become large enough to be detected as bands by Southern blotting. Peak A corresponds to smears detected as polyclonal expansion by SBH, and then peaks B, C and D appear with oligoclonal bands.

Materials and methods

Samples

Samples were collected from our ATL clinical laboratory, consisting of 16 asymptomatic and 13 symptomatic carriers and 8 patients with lymphoma-type ATL as a control because this type of ATL has no circulating ATL cells. A total of 37 samples were seropositive for HTLV-1 and undetectable morphologically and immunophenotypically for ATL cells, indicating all samples had no evidence of circulating ATL cells.

Serologic and genomic assays for HTLV-1

Anti-HTLV-1 antibodies were detected by chemiluminescent enzyme immunoassay (Fuji Rebio, Tokyo, Japan). High-molecular-weight DNA was extracted from blood mononuclear cells (MNCs) using a QIAmp DNA Blood Mini kit (Qiagen GmbH, Hilden, Germany). VL was quantified by LightCycler Technology (Roche Diagnostics KK, Tokyo, Japan) using hydro-probes and previously described primers [15], with β-globin as an internal control. The PCR methodology was monitored by determining the amount of β-globin DNA required to generate 10,000 copies per 5,000 MNC. We assumed that one infected cell harbored one provirus, and the number of infected cells was therefore estimated to be the same as the proviral copy number and was expressed per 100 MNC (% or load).

Clonal assay by SBH

SBH analysis was performed as described previously [18,19], using mixture probes covering the total region of the provirus digoxigenined and the restriction enzymes *EcoR1* and *Pst-1*. There are four *Pst-1* sites but no *EcoR1* site within the proviral sequence. Accordingly, if *EcoR1*-digestion gave no-band or faint smears and *Pst-1*-digestion gave only three internal bands, the sample was considered to be negative for clonal expansion. When discernible discrete band(s) in the *EcoR1*-digestion membrane or one or two external band(s) in addition to three internal bands in the *Pst-1*-digestion membrane were visible, the sample was considered to harbor clonal integrated provirus, implying that the infected cells had expanded clonally. The results of SBH analysis were classified into three patterns; no-band, dense smears and one or more discrete band(s). "Dense" smears were assumed to be distinct from those of common carriers (3 fold< smear density relative to background lane densitiy). The detection sensitivity for clonally infected cells in the SBH assay was 3-5% [18]. The sensitivity was monitored in each blotting membrane using 3-5% clonal cells from the ST1 ATL cell line.

Statistics

Data were analyzed using Mann-Whitney or Chi-squared tests. Statistical significance was set at $p < 0.05$.

Additional material

Additional file 1 Summary of the main clinical and laboratory data in seropsitive individuals with high VL and aberrant band patterns in SBH, and outcome in Dec 2008. Two cases (#3 and 5) among 8 advanced carriers (cases 1 to 8) developed ATL 4 and 3 years later. Cases 1, 2 and 15: High VL carriers with polyclonal expansion. Cases 3-14; aberrant bands mainly with faint multiple clonal bands, Final diagnosis was based on the integrated findings of an LN SBH test and clinico-pathological examinations. ALCL; anaplastic large cell lymphoma, DLBCL; diffuse large cell B-cell lymphoma, (-) or (+); negative or positive clonal band, S; smear, B; band, NT: not tested, Dx: diagnosis, *: indeterminate for clonal band, **: pathological diagnosis was indeterminate. For the other abbreviations; refer to the context.

Abbreviations

HTLV-1: human T-cell leukemia virus type-1; ATL: adult T-cell Leukemia; VL: HTLV-1 proviral load; SBH: Southern blot hybridization; PCR: polymerase chain reaction.

Competing interests

The authors declare that they have no competing interests.

Authors' contributions

SK, DS, and TW conceived this study and provided funding. DS, HH, KY, YY and KT collected samples and carried out the molecular genetic studies. MI, TW, AO and SK analyzed the data and discussed the results. SK organized the study and wrote the manuscript. All authors read and approved the final manuscript.

Acknowledgements

This study was supported by a Grant-in-Aid for Scientific Research (No:21390182)

Author Details

[1]Department of Laboratory Medicine, Nagasaki University Graduate School of Biomedical Sciences, Nagasaki, Japan, [2]Department of Hematology, Nagasaki University Graduate School of Biomedical Sciences, Nagasaki, Japan and [3]Graduate School of Frontier Sciences, University of Tokyo, Tokyo, Japan

Received: 25 December 2009 Accepted: 28 April 2010
Published: 28 April 2010

References

1. Poiesz BJ, Ruscetti FW, Gazdar AF, Bunn PA, Minna JD, Gallo RC: **Detection and isolation of type C retrovirus particles from fresh and cultured lymphocytes of a patient with cutaneous T-cell lymphoma.** *Proc Natl Acad Sci USA* 1980, **77**:7415-9.
2. Osame M, Usuku K, Izumo S, Ijichi N, Amitani H, Igata A, Matsumoto M, Tara M: **HTLV-I associated myelopathy, a new clinical entity.** *Lancet* 1986, **3**:1031-2.
3. Matsuoka M: **Human T-cell leukemia virus type I (HTLV-I) infection and the onset of adult T-cell leukemia (ATL).** *Retrovirology* 2005, **26(2)**:27.
4. Etoh K, Tamiya S, Yamaguchi K, Okayama A, Tsubouchi H, Ideta T, Mueller N, Takatsuki K, Matsuoka M: **Persistent clonal proliferation of human T-lymphotropic virus type I-infected cells in vivo.** *Cancer Res* 1997, **57**:4862-7.
5. Etoh K, Yamaguchi K, Tokudome S, Watanabe T, Okayama A, Stuver S, Mueller N, Takatsuki K, Matsuoka M: **Rapid quantification of HTLV-I provirus load: detection of monoclonal proliferation of HTLV-I-infected cells among blood donors.** *Int J Cancer* 1999, **81**:859-64.
6. Okayama A, Stuver S, Matsuoka M, Ishizaki J, Tanaka G, Kubuki Y, Mueller N, Hsieh CC, Tachibana N, Tsubouchi H: **Role of HTLV-1 proviral DNA load and clonality in the development of adult T-cell leukemia/lymphoma in asymptomatic carriers.** *Int J Cancer* 2004, **110(4)**:621-5.
7. Yoshida M, Seiki M, Yamaguchi K, Takatsuki K: **Monoclonal integration of human T-cell leukemia provirus in all primary tumors of adult T-cell leukemia suggests causative role of human T-cell leukemia virus in the disease.** *Proc Natl Acad Sci USA* 1984, **81**:2534-7.
8. Furukawa Y, Fujisawa J, Osame M, Toita M, Sonoda S, Kubota R, Ijichi S, Yoshida Y: **Frequent clonal proliferation of HTLV-1-infected T-cells in HAM-TSP.** *Blood* 1992, **80**:1012-6.
9. Ikeda S, Momita S, Kinoshita K, Kamihira S, Moriuchi Y, Tsukasaki K, Ito M, Kanda T, Moriuchi R, Nakamura T: **Clinical course of human T-lymphotropic virus type I carriers with molecularly detectable monoclonal proliferation of T lymphocytes: defining a low- and high-risk population.** *Blood* 1993, **82**:2017-24.
10. Matsuoka M, Tamiya S, Takemoto S, Yamaguchi K, Takatsuki K: **HTLV-I provirus in the clinical subtypes of ATL.** *Leukemia* 1997:67-9.
11. Gabet AS, Mortreux F, Talarmin A, Plumelle Y, Leclercq I, Leroy A, Gessain A, Clity E, Joubert M, Wattel E: **High circulating proviral load with oligoclonal expansion of HTLV-1 bearing T cells in HTLV-1 carriers with strongyloidiasis.** *Oncogene* 2000, **19**:4954-60.
12. Satoh M, Toma H, Sugahara K, Etoh K, Shiroma Y, Kiyuna S, Takara M, Matsuoka M, Yamaguchi K, Nakada K, Fujita K, Kojima S, Hori E, Tanaka Y, Kamihira S, Sato Y, Watanabe T: **Involvement of IL-2/IL-2R system activation by parasite antigen in polyclonal expansion of CD4 (+)25(+) HTLV-1-infected T-cells in human carriers of both HTLV-1 and S. stercoralis.** *Oncogene* 2002, **21(16)**:2466-75.
13. Wattel E, Vartanian JP, Pannetier C, Wain-Hobson S: **Clonal expansion of human T-cell leukemia virus type I-infected cells in asymptomatic and symptomatic carriers without malignancy.** *J Virol* 1995, **69(5)**:2863-8.
14. Yamaguchi K, Kiyokawa T, Nakada K, Yul LS, Asou N, Ishii T, Sanada I, Seiki M, Yoshida M, Matutes E, *et al.*: **Polyclonal integration of HTLV-I proviral DNA in lymphocytes from HTLV-I seropositive individuals: an intermediate state between the healthy carrier state and smouldering ATL.** *Br J Haematol* 1988, **68(2)**:169-74.
15. Kamihira S, Dateki N, Sugahara K, Yamada Y, Tomonaga M, Maeda T, Tahara M: **Real-time polymerase chain reaction for quantification of HTLV-1 proviral load: application for analyzing aberrant integration of the proviral DNA in adult T-cell leukemia.** *Int J Hematology* 2000, **72**:79-84.
16. Nakada K, Yamaguchi K, Furugen S, Nakasone T, Nakasone K, Oshiro Y, Kohakura M, Hinuma Y, Seiki M, Yoshida M, *et al.*: **Monoclonal integration of HTLV-I proviral DNA in patients with strongyloidiasis.** *Int J Cancer* 1987, **15;40(2)**:145-8.
17. Chen YX, Ikeda S, Mori H, Hata T, Tsukasaki K, Momita S, Yamada Y, Kamihira S, Mine M, Tomonaga M: **Molecular detection of pre-ATL state among healthy HTLV-1 carriers in an endemic area of Japan.** *Int J Cancer* 1995, **16;60(6)**:798-801.
18. Kamihira S, Sugahara K, Tsuruda K, Minami S, Uemura A, Akamatsu N, Nagai H, Murata K, Hasegawa H, Hirakata Y, Takasaki Y, Tsukasaki K, Yamada Y: **Proviral status of HTLV-1 integrated into the host genomic DNA of adult T-cell leukemia cells.** *Clin Lab Haematol* 2005, **27**:235-41.
19. Uemura A, Sugahara K, Nagai H, Murata K, Hasegawa H, Hirakata Y, Tsukasaki K, Yamada Y, Kamihira S: **An ATL cell line with an IgH pseudo-rearranged band pattern by southern blotting: a pitfall of genetic diagnosis.** *Lab Hematol* 2005, **11**:8-13.

doi: 10.1186/1743-422X-7-81
Cite this article as: Sasaki *et al.*, High Human T Cell Leukemia Virus Type-1(HTLV-1) Provirus Load in Patients with HTLV-1 Carriers Complicated with HTLV-1-unrelated disorders *Virology Journal* 2010, **7**:81

CADM1 INTERACTS WITH TIAM1 AND PROMOTES INVASIVE PHENOTYPE OF HUMAN T-CELL LEUKEMIA VIRUS TYPE I (HTLV-I) TRANSFORMED CELLS AND ADULT T-CELL LEUKEMIA (ATL) CELLS*

Mari Masuda[1,2§], Tomoko Maruyama[2,3], Tsutomu Ohta[1], Akihiko Ito[3], Tomayoshi Hayashi[4], Kunihiko Tsukasaki[5], Shimeru Kamihira[6], Shoji Yamaoka[7], Hiroo Hoshino[8], Teruhiko Yoshida[1], Toshiki Watanabe[9], Eric J. Stanbridge[10] and Yoshinori Murakami[2,3]

From [1]Genetics Division and [2]Tumor Suppression & Functional Genomics Project, National Cancer Center Research Institute, Tokyo 104-0045, Japan; [3]Division of Molecular Pathology, Department of Cancer Biology, Institute of Medical Science, The University of Tokyo, Tokyo 108-8639, Japan; [4]Department of Pathology, [5]Department of Molecular Medicine and Hematology, and [6]Department of Laboratory Medicine, Nagasaki University Graduate School of Biomedical Sciences, Nagasaki 852-8523, Japan; [7]Department of Molecular Virology, Graduate School of Medicine, Tokyo Medical and Dental University, Tokyo 113-8510, Japan; [8]Department of Virology and Preventive Medicine, Gunma University Graduate School of Medicine, Maebashi 371-8511, Japan; [9] Laboratory of Tumor Cell Biology, Department of Medical Genome Sciences, Graduate School of Frontier Sciences, The University of Tokyo, Tokyo 108-8639 and [10]Department of Microbiology and Molecular Genetics, College of Medicine, University of California, Irvine, CA, 92697, USA

Running title : Interaction of CADM1 with Tiam1 in ATL cells

To whom correspondence should be addressed: Yoshinori Murakami, Division of Molecular Pathology, Department of Cancer Biology, Institute of Medical Science, The University of Tokyo, 4-6-1 Shirokanedai, Minato-ku, Tokyo 108-8639, Japan. Tel.: +81-3-5449-5260; FAX: +81-3-5449-5407; E-mail: ymurakam@ims.u-tokyo.ac.jp

or

Mari Masuda, Chemotherapy Division, National Cancer Center Research Institute, Tokyo, 5-1-1 Tsukiji, Chuo-ku, Tokyo 104-0045, Japan. Tel.: +81-3-3542-2511, ext.3001; FAX: +81-3-3547-5298; E-mail: mamasuda@ncc.go.jp

CADM1 **encodes a multi-functional immunoglobulin-like cell adhesion molecule whose cytoplasmic domain contains a type II PSD95/Dlg/ZO-1 (PDZ)-binding motif (BM) for associating with other intracellular proteins. Although *CADM1* lacks expression in T lymphocytes of healthy individuals, it is overexpressed in adult T-cell leukemia-lymphoma (ATL) cells. It has been suggested that the expression of CADM1 protein promotes infiltration of leukemic cells into various organs and tissues which is one of the frequent clinical manifestations of ATL. Amino acid sequence alignment revealed that T-lymphoma invasion and metastasis 1 (Tiam1), a Rac-specific guanine nucleotide exchange factor (RacGEF), has a type II PDZ domain similar to those of membrane-associated guanylate kinase homologs (MAGUKs) that are known to bind to the PDZ-BM of CADM1. In this study, we demonstrated that the cytoplasmic domain of CADM1 directly interacted with the PDZ domain of Tiam1 and induced lamellipodia formation through Rac activation in HTLV-I transformed cell lines as well as ATL cell lines. Our results indicate that Tiam1 integrates signals from CADM1 to regulate the actin cytoskeleton through Rac activation. It is probable, therefore, that the CADM1-Tiam1 interaction promotes cell motility leading to tissue infiltration of leukemic cells in ATL patients.**

CADM1 is the recently unified nomenclature for *tumor suppressor in non-small cell lung cancer 1 (TSLC1)* (1) that had a variety of different names including *IGSF4A* (2), *RA175* (3), *SgIGSF* (4), *SynCAM1* (5) and *Necl-2* (6) due to its previously reported multiple functions. *CADM1* encodes an immunoglobulin-like cell adhesion molecule (IgCAM) with three immunoglobulin loops. The ectodomain of CADM1 mediates intercellular adhesion through homophilic or

heterophilic *trans*-interaction between neighboring cells (7). Despite being a tumor suppressor in various carcinomas, recent DNA microarray analysis of primary adult T-cell leukemia/lymphoma (ATL) cells from acute-type ATL patients revealed that *CADM1* was upregulated over 30-fold in those patients through an as-yet-unknown mechanism (8). ATL is a neoplastic disease of CD4 positive T lymphocytes that is etiologically associated with human T-cell leukemia virus type I (HTLV-I) (9). ATL develops in 3-5% of HTLV-I-infected individuals after an extended latent period of approximately 40-60 years (10) yet it remains an aggressive disease with poor prognosis and a median survival time of 11-13 months reported even in patients treated with the most effective first-line combination chemotherapy (11). ATL is well known for its propensity of infiltrating leukemic cells into various organs and tissues such as the skin, lungs, liver, gastrointestinal tract, central nervous system, lymph nodes and bone (12). Previous studies reported that various cell adhesion molecules, cytokines, chemokines and chemokine receptors are implicated in the process of ATL cell infiltration (13). Since cell adhesion is a critical step in tumor cell invasion, it has been proposed that over-expression of CADM1 accelerates the tissue infiltration of ATL cells (8).

The cytoplasmic domain of CADM1 contains two conserved protein-interaction modules (1). One is the submembranous protein 4.1-binding motif (protein 4.1-BM) in which members of the protein 4.1 family bind and link CADM1 to the actin cytoskeleton (14). The other is the COOH-terminal (C-terminal) EYFI sequence called type II PDZ-binding motif (PDZ-BM) in which membrane-associated guanylate kinase homologs (MAGuKs) interact through their PDZ (PSD-95, Discs large and ZO-1) domains (6,15). PDZ domains are comprised of approximately 90 amino acids and bind to the C-terminal PDZ-binding motif of target protein. Type I, II and III PDZ domains recognize E-(S/T)-X-(V/I), Φ-X-Φ and X-D-X-V, respectively, where X is any amino acid and Φ is a hydrophobic amino acid residue (16,17). Proteins harboring PDZ-BM interact with PDZ-domain-containing proteins and induce various cellular functions. One well-known example is the Tax oncoprotein encoded by HTLV-I, a key player of ATL leukemogenesis, has type I PDZ-BM, ETEV, at the C-terminus (ETEV). Tax exerts transforming activities by binding with several intracellular PDZ-domain-containing proteins (18,19), which is believed to be involved in ATL leukemogenesis. Bioinformatic analysis of the amino acid sequence revealed that T-lymphoma invasion and metastasis 1 (Tiam1) has a type II PDZ domain that shares significant similarities with those of MAGUKs. *Tiam1* was originally identified as an invasion- and metastasis-inducing gene in murine T-lymphoma cells that encodes a guanine nucleotide exchange factor (GEF) specific for Rac, a member of the Rho GTPases (20,21). Rho GTPases including Rho, Rac and Cdc42 act as molecular switches by cycling between active (GTP-bound) and inactive (GDP-bound) states to regulate actin dynamics that are involved in diverse cellular responses including cell adhesion and motility (22). The activation of Rho GTPases is mediated by specific GEFs that catalyze the exchange of GDP for GTP. In their active state, Rho GTPases bind to their effectors with high affinity thereby eliciting downstream responses (22). It has been well documented that reorganization of the actin cytoskeleton by Rho GTPases is the primary mechanism of cell motility and is essential for most types of cell migration. Among the RhoGTPases, Rac has long been known to induce the formation of actin-rich membrane ruffles or lamellipodia at the leading edge of motile cells that are required for forward movement of migratory cells (22-24). Overexpression of Tiam1 is known to increase invasion of T lymphoma cells into a fibroblast monolayer (21) as well as to induce lamellipodia formation and cell-spreading through activation of Rac. There is a growing body of evidence indicating that the interaction between GEFs and other proteins through PDZ motives is a general mechanism for controlling the exchange activity of GEFs (25). No scaffold protein or integral membrane protein has as yet been reported to associate with the PDZ domain of Tiam1 although this seems highly probable. We hypothesized, therefore, that in addition to its role as an anchor of the actin cytoskeleton to the cell membrane through protein 4.1, CADM1 is able to recruit Rac-specific GEF Tiam1 to the cell membrane and induce reorganization of the cortical actin in ATL cells thereby rendering ATL-cells motile. This

scenario could explain the invasive nature of ATL cells overexpressing CADM1.

In the present study, we have demonstrated that the cytoplasmic domain of CADM1 directly associates with Tiam1 through the PDZ domain of Tiam1 and induces lamellipodia formation through Rac activation in both HTLV-I transformed cell lines and ATL cell lines. This interaction between CADM1 and Tiam1, therefore, could play a role in infiltration of leukemic cells into various organs and tissues in ATL patients

.

Experimental Procedures

Cells - Jurkat, Molt-4, CCRF-CEM, T-all and CEM/C2 cell lines derived from acute lymphoblastic T-cell leukemia patients and H9 and Hut78 derived from cutaneous T-cell lymphoma were obtained from American Type Culture Collection (ATCC). Jurkat Tet-Off cell line was purchased from Takara Bio. HTLV-I-transformed cell lines used in this study, MT-2, MT-4, C91/PL and C8166-45, were supplied from the NIH AIDS research and reference reagent program. ATL-1K, TL-Oml and ATL-43Tb(-) cell lines were leukemic T-cell lines derived from ATL patients and provided by Masanao Miwa (Nagahama Institute of Bio-science and Technology, Nagahama, Japan), Kazuo Sugamura (Tohoku University, Sendai, Japan) and Michiyuki Maeda (Kyoto University, Kyoto, Japan), respectively. ATL-3I cell line was described previously(26). All T cell lines described above were maintained in RPMI medium (Sigma) supplemented with 10% Tet system approved FBS (Takara Bio) and 100 units/ml penicillin and 100 μg/ml streptomycin (Invitrogen). Mouse NIH3T3 fibroblasts and human embryonic kidney (HEK) 293 cells were from ATCC and grown in DMEM supplemented with 10% FBS (Sigma) and 100 units/ml penicillin and 100 μg/ml streptomycin. Normal human dermal fibroblasts (NHDF) and human adult dermal microvascular endothelial cells (HMVEC) were purchased from Lonza Walkersville Inc. and maintained in culture media specified by the manufacturer's instructions.

Antibodies and reagents - Mouse monoclonal antibodies (mAbs) specific to V5 (R960-25), CD44 (C26), Talin (8D4) and α-Tubulin (sc-8035) were obtained from Invitrogen, BD Biosciences, Sigma and Santa Cruz Biotechnology, respectively. CADM1 antibodies used in this study were rabbit polyclonal antibodies (pAbs) against the cytoplasmic domain, CC2 (7) and #6 (27); a rabbit pAb against the ectodomain, EC (28); and a chicken mAb against the ectodomain, 3E1 (29). A rabbit pAb to Tiam1 (C16) was purchased from Santa Cruz Biotechnology. Secondary antibodies used for immunoblot analysis were from GE Healthcare. For immunofluorescent staining, all fluorophore-conjugated secondary antibodies were obtained from Jackson Immuno Research Lab. Alexa Fluor 568-phalloidin or Alexa Fluor 633-phalloidin (Invitrogen) was used to visualize the actin cytoskeleton.

Construction of Expression Vectors - Full-length human Tiam1 cDNA was generated from adult human brain polyA RNA (Takara Bio) by RT-PCR using the Superscript First-Strand Synthesis System (Invitrogen) and the Expand High-Fidelity PCR system (Roche Diagnostics) and cloned into either a pcDNA3.1hygro(+) vector (Invitrogen) for expressing Tiam1 (pcDNA3.1/Tiam1) or a pcDNA3.1/V5-HIS-TOPO vector (Invitrogen) for expressing Tiam1 tagged with V5 (pcDNA3.1/Tiam1-V5). The pcDNA3.1/Tiam1-V5 was used as a template to create truncated Tiam-V5 constructs by PCR. For construction of C1199-V5 and C580-V5 mutants, the NH_2-terminal (N-terminal) 392 and 1011 amino acid residues were removed, respectively (Fig. 2C). The truncated mutant C1199ΔPDZ-V5 was designed to remove 146 amino acids (817-962) encompassing the PDZ domain from the C1199 mutant (Fig. 2C). In generating pcDNA3.1/PDZ-V5, the PDZ fragment (amino acids 817-972) of Tiam1 was amplified by PCR and subcloned into a pcDNA3.1/V5-HIS-TOPO vector. Construction of pTRE2/CADM1 expressing full-length CADM1 and pTRE2/ΔC-HA expressing CADM1 lacking its cytoplasmic tail was described previously (30). Nucleotide sequences of all PCR-amplified fragments were confirmed by sequencing. A plasmid encoding the human dominant negative mutant of Rac1, Rac1(T17N), was obtained from Upstate and the EcoRI-PmeI fragment containing the coding region of Rac1(T17N) was subcloned into a pEGFP-N3 vector at the EcoRI and SmaI sites (Takara Bio). The constructs for the N-terminal GST-tagged cytoplasmic domain of CADM1

(GST-CADM1-C) and the truncated mutant lacking the C-terminal 3 amino acids (GST-CADM1-CΔ3) were also described previously (15).

Transfection - To obtain Jurkat Tet-Off cell clones expressing full-length CADM1 or the mutant lacking the cytoplasmic domain of CADM1, cells were transfected with pTRE2/CADM1 or pTRE2/ΔC-HA using Fugene 6 (Roche Diagnostics) and selected in a medium containing 300 μg/ml hygromycin (Invitrogen). Transient transfection of HEK293 cells and T cell lines with plasmids were also performed with Fugene 6.

RNA interference - Target sequences for small interfering RNA were as follows: for human CADM1, 5'-CTGGCCCTATTTAGATGATAA-3' (CADM1siRNA#1) and 5'-AACGAAAGACGTGACAGTGAT-3' (CADM1siRNA#2); and for human Tiam1, 5'-AACATGTAGAGCACGAGTTTT-3' (Tiam1siRNA#1) and 5'-CGGCGAGCTTTAAGAAGAA-3' (Tiam1siRNA#2). The RNA duplexes (Qiagen) were introduced into cells by electroporation using a Microporator (Digital Bio Technology) according to the manufacturer's instruction. AllStars Negative Control siRNA (Qiagen) was used as the control.

Cell adhesion assay - Cell adhesion assays were performed with a Vybrant cell adhesion assay kit (Invitrogen) according to the manufacturer's protocol. Briefly, cells labeled with calcein AM were cocultured on NHDF monolayers for two hours. After removing the nonadherent cells, the absorbance at 494 nm was measured with a multilabel counter Wallac 1420 ARVOsx (PerkinElmer).

GST pulldown assay - GST-CADM1 fusion proteins expressed in *Escherichia coli* were purified with glutathione Sepharose 4B (GE Helathcare). [^{35}S]methionine-labeled full-length Tiam1 and deletion mutants were synthesized in reticulocytes using a TNT T7 Quick Coupled transcription/translation system (Promega). GST pull down assay was performed as described previously (14).

Immunoblot analysis and immunoprecipitation - Preparation of cell lysates and immunoblot analysis were described previously (7). A rabbit anti-CADM1 pAb, CC2, was used for detecting CADM1 by immunoblot analysis. For immunoprecipitation, cell lysates containing 500 μg of protein were first precleared by incubation with protein A-sepharose or protein G-sepharose (GE Helathcare) for three hours at 4°C. The precleared lysates were then incubated with a rabbit anti-CADM1 pAb, EC1, or a mouse anti-V5 mAb overnight at 4°C. A rabbit IgG or mouse IgG was used as a negative control. The protein-antibody conjugates were precipitated with protein A-sepharose or protein G-sepharose for one hour at 4°C. Immunoprecipitates were rinsed three times with the lysis buffer, fractionated either in a 4-12% gradient Nupage gel (Invitrogen) or a 3-5% Tris-actate Nupage gel (Invitrogen) and then immunoblotted.

Immunocytochemistry and Confocal Microscopy - Immunostaining and confocal microscopy with either a Carl Zeiss LSM510 or Bio-Rad Radiance 2000 Laser confocal scanning system were described previously (7,30).

Human samples and histological examination - ATL patients underwent excisional biopsies of lymph nodes at Nagasaki University Hospital from 1998 to 2006. The diagnosis of ATL was based on clinical features, hematological findings, including histologically proven mature T-cell leukemia/lymphoma and serum anti-HTLV-1 antibodies. Immunohistochemistry of formalin-fixed and paraffin-embedded tissue sections were performed as described previously(31,32).

RESULTS

Expression of CADM1 and Tiam1 in HTLV-I transformed cell lines and ATL cell lines. We first examined localization of CADM1 in HTLV-I transformed cell lines and ATL cell lines. When cultured in media, these cells tend to grow in aggregates as observed in HTLV-I transformed MT-2 cells (Fig. 1A). CADM1 was concentrated at cell-cell contact sites (Fig. 1A) indicating that homophilic *trans*-interaction of CADM1 may have promoted the formation of these cell aggregates. In epithelia, homophilic *trans*-interaction of CADM1 mediates adhesion of apposing cells (30) and the PDZ-BM of CADM1 associates with MAGuKs such as MPP3 (15), Pals2 (6) and CASK (5). It has been suggested that the interaction of CADM1 and MAGuKs plays a role in maintaining epithelial morphology (33).

In an attempt to elucidate the role of CADM1 in ATL cells, we performed database homology searches of all NCBI sequences looking for cytoplasmic proteins with type II PDZ domains similar to the PDZ domains of MAGuKs and found T-lymphoma invasion and metastasis 1 (Tiam1) which is a Rac-specific GEF. Amino acid sequence alignment revealed that among the members of MAGuKs, MPP2, Pals2 (MPP6) and CASK showed the closest similarity to the type II PDZ domain of Tiam1 (Fig. 1B). We analyzed, therefore, the expression of Tiam1 as well as CADM1 in both HTLV-I transformed cell lines and ATL cell lines. As reported in an earlier study (8), CADM1 was specifically expressed in HTLV-I transformed cell lines and ATL cell lines (Fig. 1C and Fig. S1, middle panel). In contrast, Tiam1 was detected not only in those cells, but also in cell lines derived from HTLV-I negative acute lymphoblastic T-cell leukemia and cutaneous T-cell lymphoma (Fig. 1C and Fig. S1, top panel), indicating that expression of Tiam1 is not correlated with either HTLV-I infection or ATL. The molecular weight of CADM1 varied due to the difference in N-linked and O-linked glycosylation (data not shown).

Cytoplasmic domain of CADM1 interacted with Tiam1 in HTLV-I transformed cell lines and ATL cell lines. We initially tested the physiological association of CADM1 with Tiam1 in a co-immunoprecipitation assay using an HTLV-I transformed MT-2 cell line. When endogenous CADM1 was immunoprecipitated with a rabbit anti-CADM1 pAb (EC) from the MT-2 cell lysate, co-immunoprecipitation of endogenous Tiam1 was detected (Fig. 2A). Conversely, CADM1 was specifically detected in Tiam1 immunoprecipitate (Fig. 2A). The molecular weight of CADM1 co-precipitated with Tiam1 was slightly higher than the CADM1 signal detected in the MT-2 whole cell lysate (Fig. 2A) which may suggest that Tiam1 selectively interacts with heavily glycosylated CADM1 species. Reciprocal co-precipitation of CADM1 and Tiam1 was also observed in another HTLV-I transformed cell line, C91/PL, as well as in an ATL cell line, ATL-3I (data not shown), proving that CADM1 was indeed associated with Tiam1 in those cells. N-terminal truncation of Tiam1 (C1199) (Fig. 2C, left panel) has been known to enhance its *in vitro* GEF activity and also has been suggested to increase the stability of Tiam1 due to the loss of PEST domains (Fig. 2C, left panel) that are believed to function as targeting signals to the degradation machinery (34). We examined, therefore, whether this active form of Tiam1, C1199, could associate with CADM1. A plasmid encoding either the full-length Tiam1 tagged with V5 (Tiam1-V5) or C1199 tagged with V5 (C1199-V5) was transfected into HEK293 cells and both Tiam1-V5 and C1199-V5 were immunoprecipitated with a mouse anti-V5 mAb. Endogenous CADM1 was co-immunoprecipitated not only with Tiam1-V5, but also with C1199-V5 (Fig. 2B) in HEK293 cells indicating that C1199 interacted with CADM1. We next analyzed whether Tiam1 would directly bind to the cytoplasmic domain of CADM1 by a GST pull-down assay using various truncation mutants of Tiam1 that were translated as V5-tagged proteins in rabbit reticulocyte lysates containing [$^{(35)}$S]methionine. The bacterially expressed glutathione-S-transferease (GST) protein fused with the cytoplasmic domain of CADM1 (GST-CADM1-C) was precipitated with full-length Tiam1 and C1199, but not with C580 indicating that the cytoplasmic domain of CADM1 directly interacted with Tiam1 and amino acid residues between 393 and 1012 of Tiam1 were essential for this direct interaction between CADM1 and Tiam1 (Fig. 2C and Fig. S2). We further identified the PDZ domain of Tiam1 as the region responsible for the CADM1 binding. While the PDZ tightly bound to GST-CADM1-C, deleting the PDZ domain from C1199 (C1199ΔPDZ) was enough to abolish the interaction between C1199-C5 and GST-CADM1-C (Fig. 2C and Fig S2). In contrast, GST protein fused with the cytoplasmic domain of CADM1 lacking C-terminal 3 amino acids (GST-CADM1-CΔ3) did not associate with either C1199, C580 or PDZ, thus demonstrating that the PDZ-BM of CADM1 was sufficient for the direct interaction between Tiam1 and CADM1.

Cytoplasmic domain of CADM1 induced formation of lamellipodia through Rac activation in Jurkat Tet-off cells expressing CADM1. In an attempt to assess the role of CADM1 in the infiltration of ATL cells into tissue, we established doxycycline (Dox)-inducible acute lymphoblastic T-cell leukemia Jurkat cell clones expressing

CADM1 (Jurkat/CADM1). In the isolated Jurkat/CADM1 cell clone, expression of CADM1 was tightly regulated with Dox (Fig. 3A). Expression of CADM1 induced extensive formation of cell aggregates in Jurkat cells (Fig. 3A, bottom right panel) that were reminiscent of cell aggregates seen in HTLV-I transformed cell lines, such as MT-2 cells (Fig. 1A), and ATL cell lines indicating that homophilic *trans*-interaction of CADM1 mediated formation of cell aggregates in Jurkat cells. It appears that homophilic *trans*-interaction of CADM1, therefore, contributes to formation of aggregates in many of the HTLV-I transformed cell lines and ATL cell lines. In Jurkat/CADM1 cells, co-immunoprecipitation of endogenous Tiam1 was also confirmed in the precipitate with anti-CADM1 pAb (EC) (Fig. 3B). We next examined localization of CADM1 and Tiam1 in Jurkat/CADM1 cells co-cultured on a monolayer of mouse NIH3T3 fibroblasts for seven hours. In the absence of Dox, Jurkat cells expressing CADM1 tightly adhered to and spread over the monolayer of fibroblasts forming lamellipodia where CADM1 and Tiam1 were colocalized (Fig. 3C, middle and bottom panels). In contrast, Jurkat/CADM1 cells in which CADM1 expression was repressed with Dox neither infiltrated into the monolayer of fibroblasts nor formed membrane ruffles at the cell edge and Tiam1 was distributed in the cytoplasm of those cells (Fig. 3C, top panels). These findings together demonstrated that CADM1 could induce lamellipodia formation and recruit Tiam1 at the periphery of the lamellipodia. Such effects by CADM1 required its cytoplasmic domain because the deletion mutant lacking the cytoplasmic domain of CADM1 could not induce lamellipodia formation in Jurkat cells co-cultured on the monolayer of fibroblasts (Fig. 3D). In addition, Tiam1 did not accumulate at the cell periphery of these cells suggesting that the interaction of the cytoplasmic domain of CADM1 and Tiam1 was necessary for the lamellipodia formation (Fig. 3D). As Tiam1 is known to be a Rac-specific GEF, we also tested whether activation of Rac was needed for CADM1-induced lamellipodia formation by introducing a dominant negative mutant of Rac tagged with GFP (T17NRac1-GFP) in Jurkat/CADM1 cells. T17NRac1-GFP completely blocked CADM1-induced lamellipodia formation (Fig. 3E) thereby underscoring the importance of Rac activation presumably through Tiam1 in CADM1-induced lamellipodia formation.

CADM1 and Tiam1 colocalized at the leading edge of migrating ATL-3I cells. Infiltration of ATL cells into various kinds of tissue like skin involves several key steps: 1) adhesion to endothelial cells; 2) transmigration of vessel walls; 3) crawling into dermis where fibroblasts are abundant; and 4) epidermal localization. We looked, therefore, into the localization of CADM1 and Tiam1 in ATL cell lines co-cultured on either human dermal microvascular endothelial cells (HMVEC) or normal human dermal fibroblasts (NHDF). After 17 hours co-culture of the ATL cell line, ATL-3I, on top of the monolayer of HMVEC, the cells firmly adhered to HMVEC and formed lamellipodia where CADM1 and Tiam1 were intensely co-accumulated (Fig. 4A and Fig. S3). ATL-3I cells adhered to an NHDF monolayer in shorter six-hour co-culture (Fig. 4C, D) and exhibited lamellipodia in most of the cells adhered to NHDF where colocalization of CADM1 and Tiam1 was seen (Fig. 4D). As observed in Jurkat/CADM1 cells overlaid on NIH3T3 cells, a dominant negative T17NRac1 mutant also inhibited the lamellipodia formation of ATL-3I cells on HMVEC suggesting that Rac activity was required for ATL-3I cells to tightly attach to the monolayer of HMVEC and subsequently form lamellipodia (Fig. 4B). We realize that the first requirement for a cell to initiate migration is the acquisition of polarized morphology and establishment of cell polarity occurs during the migration of lymphocytes (35). In ATL-3I cells adhered to NHDF, therefore, we compared the distribution of CADM1 to Talin and CD44 which are well-established markers for the leading and trailing edges of chemokine-induced migratory T lymphocytes, respectively. XZ cross section analysis of these cells revealed that intense staining of CADM1 and Talin was detected at the contact zones of ATL-3I cells to NHDF (Fig. 4C, *a-c*). In contrast, CD44 was not observed in those contact regions (Fig. 4C, *d-f*), indicative of CADM1 localization at the leading edge of the migrating cells. Triple immunofluorescence staining for CADM1, Tiam1 and CD44 in the XZ cross section of such cells revealed that CADM1 was completely colocalized with Tiam1 at the cell periphery (Fig. 4D, *a-d* and *e-h*). At the

adhering sites of ATL-3I cells to NHDF, however, CADM1 was colocalized with Tiam1, but not with CD44 (Fig. 4D, *a-d* and *e-h*) demonstrating that CADM1 and Tiam1 were distributed at the leading edge of polarized migrating cells. This was further confirmed by quantitative analysis of the XZ cross sections of the adhering area of ATL-3I cells to NHDF monolayers. Thirty-seven of 40 (93%) ATL-3I cells showed CADM1/Tiam1 double-positive and CD44 negative adhering sites.

Both CADM1 and Tiam1 were necessary for lamellipodia formation of HTLV-I transformed and ATL cell lines. To further substantiate the importance of CADM1 and Tiam1 in CADM1-induced lamellipodia formation, we introduced either CADM1 or Tiam1 siRNA into HTLV-I transformed cell lines, C91/PL and MT-4, and an ATL cell line, ATL-3I. Immunoblot analysis of CADM1 and Tiam1 protein revealed that decreases in CADM1 and Tiam1 were most prominent in C91/PL cells (Fig. 5A) due to them having the highest transfection efficiency among the three cell lines (data not shown). Forty-eight hours after the introduction of siRNA, the cells in which CADM1 expression had been knocked down lost their aggregate morphology and started growing as single cells (Fig. 5B, upper middle and right panels) whereas siRNA-mediated knockdown of Tiam1 interfered with aggregate formation to a much lesser extent (Fig. 5B, bottom panels). It should be noted that disruption of cell aggregation in ATL3I cells by CADM1 knockdown was not as striking as in MT-4 cells (data not shown), suggesting that other adhesion molecules are also involved in cell aggregation of HTLV-I transformed cell lines and ATL cell lines. In assessing whether the reduction in aggregate formation influenced cell growth, we counted the number of living cells seven days after siRNA introduction and found that knockdown of CADM1 dramatically reduced cell growth of C91/PL cells to approximately 30% (Fig. 5C). Although not as strongly as in C91/PL cells, cell growth of MT-4 and ATL-3I cells was also decreased from 50 to 66% upon silencing CADM1 (Fig. 5C). In contrast, knockdown of Tiam1 did not affect cell growth at levels comparable to those induced by knockdown of CADM1 (Fig. 5C). Together, these indicate that CADM1 enhanced the cell growth of both HTLV-I transformed cell lines and an ATL cell line by mediating formation of cell aggregates through homophilic *trans*-interaction of CADM1, but it is unlikely that Tiam1 was involved in the effect. We further analyzed whether CADM1 or Tiam1 was necessary for adhesion to NHDF and subsequent formation of lamellipodia on NHDF. An adhesion assay of a two-hour co-culture of these ATL cell lines on an NHDF monolayer showed that knockdown of either CADM1 or Tiam1 reduced the level of cell adhesion by a similar amount (50-70%) (Fig. 5D). This result was consistent with the immunoflurecent microscopic observation which showed that siRNA-mediated knockdown of CADM1 and Tiam1 in C91/PL cells on NHDF repressed lamellipodia formation and abrogated cell periphery localization of Tiam1 and CADM, respectively (Fig. 5E). These data together indicate that either Tiam1 or CADM1 are necessary for lamellipodia formation in HTLV-I transformed cell lines and ATL cell lines.

Colocalization of CADM1 and Tiam1 in lymph node lesions of ATL patients. Finally, we examined the expression of CADM1 and Tiam1 in lymph node lesions from nine ATL patients with lymph nodes involvement by immunohistochemistry. As representatively shown in Fig. 6A, infiltrating tumor cells demonstrated immunoreactivity for CADM1 in eight out of the nine patients tested (four strongly positive, four positive and one negative). In comparison, Tiam1 was detected in three patients who also were positive for CADM1 indicating that one-third of the specimens from those nine ATL patients were double-positive. Immunohistostaining revealed that CADM1 was detected at the plasma membrane of the tumor cells (Fig. 6A, left column) and aggregate accumulation of CADM1 was seen in some cases as an intense punctate structure (Fig. 6A, bottom left panel). Tiam1 was observed not only at the membrane, but also in the cytoplasm of the infiltrating ATL cells (Fig. 6A, right column). In an effort to determine more precisely whether CADM1 and Tiam1 colocalize, we performed immunofluorescence double-staining. Although none of the Tiam1-positive specimens showed a unique pattern of punctate structure-like distribution of CADM1 as seen in Fig. 6A, CADM1 and Tiam1 were well colocalized at the cell membrane of ATL cells (Fig. 6B). When considered together, these

data support our finding *in vitro* that both CADM1 and Tiam1 are cooperatively involved in the infiltration of ATL cells.

DISCUSSION

In this study, we identified Rac-specific GEF, Tiam1, as a binding partner of CADM1 in both HTLV-I transformed and ATL-derived cell lines and demonstrated that the interaction induced formation of lamellipodia, a structure seen at the leading edge of motile cells, indicating that CADM1-Tiam1 interaction was involved in the infiltrative propensity of ATL cells. Although the cohort of ATL patients we investigated was not large enough to provide conclusive clinical evidence, CADM1 and Tiam1 were well colocalized at the cell membrane in the $Tiam1^{+}/CADM1^{+}$ specimens from ATL patients with lymph node involvement. In normal T lymphocytes in which CADM1 is barely detectable (8), Tiam1 regulates chemokine-induced T-cell polarization and chemotaxis by associating with the Par3–Par6–aPKC polarity complex (36). In ATL cells, the overexpressed CADM1 interacts with Tiam1 through the type II PDZ-BM of CADM1 and recruits Tiam1 to the intracellular submembranous domain. RacGEF activity of Tiam1 is known to depend on Tiam1's membrane localization mediated by binding to phosphoinositides (PI) through the N-terminal Pleckstrin homology domain (PHn) of Tiam1 (Fig. 1B) (37). Others have reported, however, that the PHn of Tiam1 possesses a relatively weak affinity and less specificity for PI compared to the PH domains of PLCδ and Akt (38) indicating that binding of the PHn with PI seems to play an accessory, but not a defining role in targeting Tiam1 to cell membranes. It is, therefore, likely that the interaction of Tiam1 with transmembrane proteins facilitates its membrane localization. Furthermore, these transmembrane proteins with which Tiam1 interacts may determine the downstream signals subsequently triggered by such interaction. Accordingly, the association of CADM1 with the PDZ domain of Tiam1 could reinforce tethering of Tiam1 to the membrane and induce the signal specific to CADM1. We have previously shown that CADM1 binds to actin through its protein 4.1-BM (14). CADM1, therefore, seems to recruit actin and a regulator of actin, RacGEF, together to the juxtamembrane region thereby becoming a powerful driving force for actin reorganization to induce cell motility (Fig. 7). As can be surmised, co-expression of CADM1 and Tiam1 in T lymphocytes appears to be an unwanted combination that leads to the deviated invasive tendencies of ATL cells.

Regardless of its tumor suppressor activities in various cancers (1,33), our study revealed that CADM1 functions rather as an oncoprotein in ATL. Intriguingly, similar complexity of paradoxical functions has been well illustrated in Tiam1 (39). Besides promoting invasion of T-cell lymphoma cells (20,40), Tiam1 expression has been demonstrated to correlate with the invasive and metastatic phenotypes of breast and colon cancers (39). It has also been shown that Tiam1-/- mice are resistant to the development of Ras-induced skin tumors suggesting that Tiam1 contributes to tumorigenicity (41). As opposed to these abilities of Tiam1 to promote invasion and metastasis as well as tumor formation, Tiam1 expression has been demonstrated to be inversely correlated with invasive potential of renal cell carcinoma cell lines (42). Such contradictory findings are proposed to be due to the effects of Tiam1 which solely depend on the cell type and the RhoGTPases activation status in the particular spatio-temporal context of given cells (39). It is plausible, therefore, that the dualistic effects of CADM1 may be also attributed to the cell type and activation state of RhoGTPs. In fact, we previously demonstrated using epithelial Madin-Darby canine kidney (MDCK) cells that the cytoplasmic domain of CADM1 induced prolonged activation of Rac and reduced activation of Rho leading to suppression of hepatocyte growth factor (HGF)-induced epithelial mesenchymal transitions (EMT) which is a crucial step for tumor cells to become invasive (30). Coincidentally, ectopic expression of Tiam1 or constitutively active Rac was reported to block HGF-induced cell scattering of MDCK cells with high Rac and low Rho activities(43). It is tempting to speculate, therefore, that CADM1 spatiotemporally associates with Tiam1 even in some epithelial cells where they cooperatively work together as a tumor suppressor by maintaining epithelial integrity.

Although it is becoming increasingly clear that adhesion molecules are involved in transendothelial migration of leukocytes, this may not be the only possible process in which

CADM1 is involved in infiltration of ATL cells into various organs and tissues, such as skin. Skin involvement is one of the most frequent manifestations in ATL patients. The extracellular domain of CADM1 is known to interact homophilically with itself (6,7), as well as heterophilically with CADM2 (Necl-3) (44), CADM3 (Necl-1) (6), Nectin-3 (6) and CRTAM (45-47). The molecular interactions that facilitate ATL migration to and retention in skin may involve various cells residing in the skin that express those ligands for CADM1. Such cells may include mast cells that are immune cell residents of the dermis constitutively expressing CADM1 (48). Our study revealed that ATL cells adhered to NHDF with even higher affinity than to HMVEC. NHDF are abundant in epidermis and quite possibly help ATL cells to crawl into the dermal interstitium. We have found that CADM1-positive cells tend to show a high affinity to fibroblasts, which are CADM1 negative, suggesting that fibroblasts express some of those heterophilic ligands described above or as-yet-unidentified ligands for CADM1. ATL cells often display an affinity for Langerhans' cells, immature dermal dendritic cells, and cluster around them in the epidermis forming Pautrier's microabscesses (49). Since CADM1 is known to define a certain subset of dendritic cells (45), it is possible that Langerhans' cells express CADM1 thereby attracting ATL cells to the epidermis. It is noteworthy that the dermis is abundant in sensory nerve fibers that constitute an elaborate network. Other than CRTAM, the CADM1 ligands listed above are copiously expressed in nerve cells (5,44). It seems plausible, therefore, that ATL infiltration into skin is promoted through the interaction between ATL cells and nerve fibers. It remains elusive, however, whether the CADM1-Tiam1-Rac cascade is constitutively activated in ATL cells or the activation is triggered by adhesion of ATL cells to the cells expressing those CADM1 ligands mentioned above. Further studies to define the mechanism of CADM1 activation of Rac through Tiam1 are now ongoing. As phosphorylation of Tiam1 on its serine/threonine and tyrosine residues were previously reported (34,39), investigating spatio-temporal phosphorylation of Tiam1 in HTLV-I transformed and ATL-derived cell lines would provide pivotal information toward understanding the CADM1-Tiam1-Rac signaling in ATL cells.

In the present study, we found that CADM1-knockdown affected cell growth, suggesting that CADM1 may play an auxiliary role in transformation of HTLV-I-infected T cells. During such transformation stage, Tiam1 may not be the sole binding partner of CADM1 because Tiam1-knockdown did not have an effect on cell growth. Tax is reported to be directly associated with small Rho GTPase, therefore believed to play a role in the infiltrating propensity of ATL cells (18,50). It is known, however, that Tax expression is frequently lost in ATL cells (51). In contrast, previous study from others reported that CADM1 was expressed in all the primary ATL cells they tested (8). In such Tax-negative ATL cells, CADM1-Tiam1 interaction may become one of the driving forces for cytoskeletal reorganization, thereby contributing to the infiltrating phenotype of ATL cells. In support of this, it has been reported that compared to ED, the CADM1-nagative ATL cell line, ED cells overexpressing CADM1 caused larger tumor formation and massive infiltration into various organs in NOG mice (52).

Elucidating the molecular mechanisms of the CADM1-Tiam1 pathway involved in tissue infiltration of ATL cells may offer alternative approaches to the treatment of ATL such as specific interference with CADM1 using a monoclonal antibody (mAb) against the ectodomain of CADM1. The use of therapeutic mAb for the treatment of cancer has shown promising results over the past few years as exemplified by the major success of a mAb against HER2 in treatments for metastatic breast cancer and lung cancer. Our study revealed that CADM1 affected both lamellipodia formation and cell growth thus suggesting that interference with CADM1 may inhibit not only tissue infiltration of ATL cells, but also the growth of ATL cells. Tiam1 may also become an attractive pharmacological target for developing small-molecular inhibitors of the invasive nature of ATL cells by manipulating the CADM1-Tiam1-Rac signaling pathways.

REFERENCES

1. Kuramochi, M., Fukuhara, H., Nobukuni, T., Kanbe, T., Maruyama, T., Ghosh, H. P., Pletcher, M., Isomura, M., Onizuka, M., Kitamura, T., Sekiya, T., Reeves, R. H., and Murakami, Y. (2001) *Nat Genet* **27**, 427-430
2. Gomyo, H., Arai, Y., Tanigami, A., Murakami, Y., Hattori, M., Hosoda, F., Arai, K., Aikawa, Y., Tsuda, H., Hirohashi, S., Asakawa, S., Shimizu, N., Soeda, E., Sakaki, Y., and Ohki, M. (1999) *Genomics* **62**, 139-146
3. Urase, K., Soyama, A., Fujita, E., and Momoi, T. (2001) *Neuroreport* **12**, 3217-3221
4. Wakayama, T., Ohashi, K., Mizuno, K., and Iseki, S. (2001) *Mol Reprod Dev* **60**, 158-164
5. Biederer, T., Sara, Y., Mozhayeva, M., Atasoy, D., Liu, X., Kavalali, E. T., and Sudhof, T. C. (2002) *Science* **297**, 1525-1531
6. Shingai, T., Ikeda, W., Kakunaga, S., Morimoto, K., Takekuni, K., Itoh, S., Satoh, K., Takeuchi, M., Imai, T., Monden, M., and Takai, Y. (2003) *J Biol Chem* **278**, 35421-35427
7. Masuda, M., Yageta, M., Fukuhara, H., Kuramochi, M., Maruyama, T., Nomoto, A., and Murakami, Y. (2002) *J Biol Chem* **277**, 31014-31019
8. Sasaki, H., Nishikata, I., Shiraga, T., Akamatsu, E., Fukami, T., Hidaka, T., Kubuki, Y., Okayama, A., Hamada, K., Okabe, H., Murakami, Y., Tsubouchi, H., and Morishita, K. (2005) *Blood* **105**, 1204-1213
9. Yasunaga, J., and Matsuoka, M. (2007) *Rev Med Virol* **17**, 301-311
10. Tajima, K. (1990) *Int J Cancer* **45**, 237-243
11. Yamada, Y., Tomonaga, M., Fukuda, H., Hanada, S., Utsunomiya, A., Tara, M., Sano, M., Ikeda, S., Takatsuki, K., Kozuru, M., Araki, K., Kawano, F., Niimi, M., Tobinai, K., Hotta, T., and Shimoyama, M. (2001) *Br J Haematol* **113**, 375-382
12. Matsuoka, M. (2005) *Retrovirology* **2**, 27
13. Yoshie, O. (2005) *Leuk Lymphoma* **46**, 185-190
14. Yageta, M., Kuramochi, M., Masuda, M., Fukami, T., Fukuhara, H., Maruyama, T., Shibuya, M., and Murakami, Y. (2002) *Cancer Res* **62**, 5129-5133
15. Fukuhara, H., Masuda, M., Yageta, M., Fukami, T., Kuramochi, M., Maruyama, T., Kitamura, T., and Murakami, Y. (2003) *Oncogene* **22**, 6160-6165
16. Songyang, Z., Fanning, A. S., Fu, C., Xu, J., Marfatia, S. M., Chishti, A. H., Crompton, A., Chan, A. C., Anderson, J. M., and Cantley, L. C. (1997) *Science* **275**, 73-77
17. Sheng, M., and Sala, C. (2001) *Annu Rev Neurosci* **24**, 1-29
18. Boxus, M., Twizere, J. C., Legros, S., Dewulf, J. F., Kettmann, R., and Willems, L. (2008) *Retrovirology* **5**, 76
19. Ishioka, K., Higuchi, M., Takahashi, M., Yoshida, S., Oie, M., Tanaka, Y., Takahashi, S., Xie, L., Green, P. L., and Fujii, M. (2006) *Retrovirology* **3**, 71
20. Habets, G. G., Scholtes, E. H., Zuydgeest, D., van der Kammen, R. A., Stam, J. C., Berns, A., and Collard, J. G. (1994) *Cell* **77**, 537-549
21. Michiels, F., Habets, G. G., Stam, J. C., van der Kammen, R. A., and Collard, J. G. (1995) *Nature* **375**, 338-340
22. Ridley, A. J. (2006) *Trends Cell Biol* **16**, 522-529
23. Burridge, K., and Wennerberg, K. (2004) *Cell* **116**, 167-179
24. Malliri, A., and Collard, J. G. (2003) *Curr Opin Cell Biol* **15**, 583-589
25. Garcia-Mata, R., and Burridge, K. (2007) *Trends Cell Biol* **17**, 36-43
26. Hoshino, H., Esumi, H., Miwa, M., Shimoyama, M., Minato, K., Tobinai, K., Hirose, M., Watanabe, S., Inada, N., Kinoshita, K., Kamihira, S., Ichimaru, M., and Sugimura, T. (1983) *Proc Natl Acad Sci U S A* **80**, 6061-6065
27. Wakayama, T., Koami, H., Ariga, H., Kobayashi, D., Sai, Y., Tsuji, A., Yamamoto, M., and Iseki, S. (2003) *Biol Reprod* **68**, 1755-1763
28. Mao, X., Seidlitz, E., Ghosh, K., Murakami, Y., and Ghosh, H. P. (2003) *Cancer Res* **63**, 7979-7985
29. Furuno, T., Ito, A., Koma, Y., Watabe, K., Yokozaki, H., Bienenstock, J., Nakanishi, M., and Kitamura, Y. (2005) *J Immunol* **174**, 6934-6942
30. Masuda, M., Kikuchi, S., Maruyama, T., Sakurai-Yageta, M., Williams, Y. N., Ghosh, H. P., and Murakami, Y. (2005) *J Biol Chem* **280**, 42164-42171
31. Ito, A., Okada, M., Uchino, K., Wakayama, T., Koma, Y., Iseki, S., Tsubota, N., Okita, Y.,

and Kitamura, Y. (2003) *Lab Invest* **83**, 1175-1183
32. Ito, A., Nishikawa, Y., Ohnuma, K., Ohnuma, I., Koma, Y., Sato, A., Enomoto, K., Tsujimura, T., and Yokozaki, H. (2007) *Hepatology* **45**, 684-694
33. Murakami, Y. (2005) *Cancer Sci* **96**, 543-552
34. Mertens, A. E., Roovers, R. C., and Collard, J. G. (2003) *FEBS Lett* **546**, 11-16
35. Sanchez-Madrid, F., and del Pozo, M. A. (1999) *EMBO J* **18**, 501-511
36. Gerard, A., Mertens, A. E., van der Kammen, R. A., and Collard, J. G. (2007) *J Cell Biol* **176**, 863-875
37. Michiels, F., Stam, J. C., Hordijk, P. L., van der Kammen, R. A., Ruuls-Van Stalle, L., Feltkamp, C. A., and Collard, J. G. (1997) *J Cell Biol* **137**, 387-398
38. Ceccarelli, D. F., Blasutig, I. M., Goudreault, M., Li, Z., Ruston, J., Pawson, T., and Sicheri, F. (2007) *J Biol Chem* **282**, 13864-13874
39. Minard, M. E., Kim, L. S., Price, J. E., and Gallick, G. E. (2004) *Breast Cancer Res Treat* **84**, 21-32
40. Stam, J. C., Michiels, F., van der Kammen, R. A., Moolenaar, W. H., and Collard, J. G. (1998) *EMBO J* **17**, 4066-4074
41. Malliri, A., van der Kammen, R. A., Clark, K., van der Valk, M., Michiels, F., and Collard, J. G. (2002) *Nature* **417**, 867-871
42. Engers, R., Zwaka, T. P., Gohr, L., Weber, A., Gerharz, C. D., and Gabbert, H. E. (2000) *Int J Cancer* **88**, 369-376
43. Hordijk, P. L., ten Klooster, J. P., van der Kammen, R. A., Michiels, F., Oomen, L. C., and Collard, J. G. (1997) *Science* **278**, 1464-1466
44. Fogel, A. I., Akins, M. R., Krupp, A. J., Stagi, M., Stein, V., and Biederer, T. (2007) *J Neurosci* **27**, 12516-12530
45. Galibert, L., Diemer, G. S., Liu, Z., Johnson, R. S., Smith, J. L., Walzer, T., Comeau, M. R., Rauch, C. T., Wolfson, M. F., Sorensen, R. A., Van der Vuurst de Vries, A. R., Branstetter, D. G., Koelling, R. M., Scholler, J., Fanslow, W. C., Baum, P. R., Derry, J. M., and Yan, W. (2005) *J Biol Chem* **280**, 21955-21964
46. Boles, K. S., Barchet, W., Diacovo, T., Cella, M., and Colonna, M. (2005) *Blood* **106**, 779-786
47. Arase, N., Takeuchi, A., Unno, M., Hirano, S., Yokosuka, T., Arase, H., and Saito, T. (2005) *Int Immunol* **17**, 1227-1237
48. Ito, A., Jippo, T., Wakayama, T., Morii, E., Koma, Y., Onda, H., Nojima, H., Iseki, S., and Kitamura, Y. (2003) *Blood* **101**, 2601-2608
49. Ishida, T., and Ueda, R. (2006) *Cancer Sci* **97**, 1139-1146
50. Wu, K., Bottazzi, M. E., de la Fuente, C., Deng, L., Gitlin, S. D., Maddukuri, A., Dadgar, S., Li, H., Vertes, A., Pumfery, A., and Kashanchi, F. (2004) *J Biol Chem* **279**, 495-508
51. Matsuoka, M. (2003) *Oncogene* **22**, 5131-5140
52. Dewan, M. Z., Takamatsu, N., Hidaka, T., Hatakeyama, K., Nakahata, S., Fujisawa, J., Katano, H., Yamamoto, N., and Morishita, K. (2008) *J Virol* **82**, 11958-11963

FOOTNOTES

* This work was supported by a Grant-in-Aid for Scientific Research on Priority Areas for Cancer (No. 17015048 for Y.M.) from the Ministry of Education, Culture, Sports, Science, and Technology, Japan; a Grant-in-Aid for the Third Term Comprehensive Control Research for Cancer from the Ministry of Health, Labor, and Welfare, Japan (Y.M.); and a Grant for the Promotion of Fundamental Studies in Health Sciences from the National Institute of Biomedical Innovation (ID 05-10 for Y.M.). The authors have declared no conflict of interest.

§ Present address: Chemotherapy Division, National Cancer Center Research Institute, Tokyo, 5-1-1 Tsukiji, Chuo-ku, Tokyo 104-0045, Japan

The abbreviations used include: HTLV-I, human T-cell leukemia virus type I; ATL, adult T-cell

leukemia/lymphoma; GEF, guanine nucleotide exchange factor; IgCAMs, immunoglobulin superfamily cell adhesion molecules; PDZ, PSD95/Dlg/ZO-1; DH, dbl homology; GST, glutathione S-transferase; MAGuK, membrane-associated guanylate kinase homolog; BM, binding motif; Dox, doxycycline; mAb, monoclonal antibody; pAb, polyclonal antibody; PI, phosphoinositide; PH, pleckstrin homology; PHn, N-terminal PH domain; GFP, green fluorescent protein.

ACKNOWLEDGMENTS

We thank Haruka Kawanabe for her technical assistance. We express our gratitude to Drs. Tesshi Yamada, Yoshinori Ino and Kazufumi Honda for their generous help with the Bio-Rad Radiance 2000 confocal system. We are also grateful to Dr. Laurent Galibert for his fruitful discussion and Christopher S. Dix for his critical reading of the manuscript.

FIGURE LEGENDS

Figure 1. Expression of CADM1 and Tiam1 in HTLV-I transformed cell lines and ATL cell lines. ***A.*** Expression of CADM1 in the HTLV-I transformed cell line. MT-2 cells were immunostained for CADM1 (green) and α-tubulin (red) with a rabbit anti-CADM1 pAb (CC2) and a mouse anti-α-tubulin mAb and examined by confocal microscopy. Scale bar, 10 μm. Note that CADM1 is concentrated at the cell-cell attachment sites of the MT-2 cells. ***B.*** Schematic representation of the domain structure of Tiam1 and sequence alignment of type II PDZ domains of selected MAGuKs and Tiam1. Tiam1 contains myr, myristoylation signal; P, Pest region; PHn, N-terminal pleckstrin homology domain; RBD, Ras-binding domain; PDZ, type II PDZ (PSD-95/Dlg/ZO-1) domain; DH, dbl homology domain (the catalytic domain) and PHc, C-terminal pleckstrin homology domain. Sequences were aligned using CLUSTALW (http://align.genome.jp). Conserved residues have been highlighted in red and semi-conserved residues in green (very similar) and yellow (similar). The secondary structure elements, β-sheet and α-helix, are indicated as β and α. The GeneBank database accession numbers for the nucleotide sequences that encode human MPP2, MPP6, CASK and Tiam1 are BC030287, NM016447, AF032119 and NM003253, respectively. ***C.*** Immunoblot analysis for the expression of CADM1 and Tiam1 in acute lymphatic leukemia (ALL) cell lines, HTLV-I transformed cell lines and ATL cell lines. Five μg of cell lysates were fractionated in a 4-12% gradient NuPAGE Norvex Bis-Tris gel followed by immunoblot analysis as described in the "Experimental Procedures" section. The antibodies used were a rabbit anti-Tiam1 pAb (C16) and a rabbit anti-CADM1 pAb (CC2). A mouse anti-α-tubulin mAb was used to show a loading control.

Figure 2. Direct interaction of CADM1 with Tiam1. ***A.*** Reciprocal coimmunoprecipitation of CADM1 with Tiam1 in the HTLV-I transformed cell line, MT-2. Five hundred μg of cell lysates were immunoprecipitated (IP) with a rabbit anti-CADM1 pAb (EC), a rabbit anti-Tiam1 pAb (C16) or normal rabbit IgG. The precipitates were subjected to immunoblot analysis with the rabbit anti-Tiam1 pAb (top panel) and a rabbit anti-CADM1 pAb (CC2) (bottom panel). Red, blue and black arrows indicate Tiam1, CADM1 and the rabbit IgG heavy chain, respectively. ***B.*** Interaction of CADM1 with the active form of Tiam1 (C1199). Five hundred μg of cell lysates from HEK293 cells transiently transfected with pcDNA3.1, pcDNA/Tiam1-V5 or pcDNA/C1199-V5 were immunoprecipitated (IP) with a mouse anti-V5 mAb or normal mouse IgG and subjected to immunoblot analysis with CC2 (top panel). Five μg of whole cells lysates (WCL) were also analyzed for expression of CADM1 (middle panel), Tiam1-V5 and C1199-V5 (bottom panel) by immunoblot analysis with CC2 and anti-V5 mAb, respectively. ***C.*** The PDZ domain of Tiam1 is required for binding to the PDZ-BM of CADM1. The domain structure and truncated constructs of Tiam1 are shown on the left. GST, GST-fused with the cytoplasmic domain of TSLC1, aa392-442 (GST-CADM1-C), and GST fused with the cytoplasmic domain lacking c-terminal 3 amino acid residues, aa392-439 (GST-CADM1-CΔ3), were expressed in *Escherichia coli*. [^{35}S]Methionine-labeled full-length and truncated Tiam1 were synthesized in reticulocytes. Size of the *in vitro*-translated (IVT) proteins is shown in the right panel with dots indicating each

full-length IVT product. For *in vitro* binding, labeled proteins were incubated with GST or GST-fusion protein immobilized on glutathione Sepharose beads and subjected to SDS-PAGE. Binding of ^{35}S-labeled proteins was detected by autoradiography (middle column). The entire images of GST pulldown assay is shown in Figure S2.

Figure 3. The cytoplasmic domain of CADM1 is necessary for lamellipodia formation in tet-off Jurkat cells cultured on NIH3T3 fibroblasts. ***A.*** Inducible expression of CADM1 in tet-off Jurkat cells. The established tet-off Jurkat cell clones, Jurkat/vector and Jurkat/CADM1, were cultured in the presence (+) and absence (-) of 100 μg/ml doxycycline (Dox) for five days. Five μg of cell lysates were subjected to immunoblot analysis with an anti-CADM1 pAb (CC2) and anti-Tiam1 pAb (C16) as shown in the upper panel. Red and blue arrows indicate Tiam1 and CADM1, respectively. Representative phase-contrast images of Jurkat/CADM1 cells cultured in media with or without 100 μg/ml Dox for five days are shown in the lower panels. Original magnification, 100x. Note that CADM1-expressing Jurkat/CADM1 cells show extensive aggregates. ***B.*** Coimmunoprecipitation of CADM1 with Tiam1 in the tet-off Jurkat/CADM1 cells. The Jurkat/CADM1 cells were cultured in the presence (+) and absence (-) of 100 μg/ml Dox for five days. To confirm the expression of Tiam1 and CADM1, five μg of whole cell lystates (WCL) were subjected to immunoblot analysis (left-half panels). Five hundred μg of cell lysates were immunoprecipitated (IP) with an anti-CADM1 pAb (EC) and subjected to immunoblot analysis for Tiam1 with C16 (right-half top panel) and for CADM1 with CC2 (right-half bottom panel). Coprecipitated Tiam1 is indicated with a black arrowhead. Red and blue arrows indicate Tiam1 and CADM1, respectively. ***C.*** CADM1 is necessary for formation of lamellipodia in Jurkat cells cultured on NIH3T3 fibroblasts. Jurkat/CADM1 cells were cocultured on a monolayer of NIH3T3 cells for 17 hours. The cells were stained for CADM1 (blue) and Tiam1 (green) with a chicken anti-CADM1 mAb (3E1) and an anti-Tiam1 pAb (C16), respectively. Magnified images show that CADM1 and Tiam1 are detected at membrane ruffling areas (middle and bottom panels). Scale bar, 10 μm. ***D.*** Cytoplasmic domain of CADM1 induces formation of lamellipodia. Jurkat/CADM1 and Jurkat/ΔC-HA were seeded on NIH3T3 monolayers and incubated for 17 hours. Cells were triple-stained for CADM1 (green), Tiam1 (red) and actin (blue). Actin filaments are shown in the merged panels. Note that stress fibers of NIH3T3 cells are seen in the top merged panel indicating that Jurkat/CADM1 cells infiltrated into the NIH3T3 monolayer. Scale bar, 10 μm. ***E.*** A dominant negative mutant of Rac1, T17NRac1, blocked CADM1-induced lamellipodia formation. Jurkat/CADM1 cells cultured in the presence (+) or absence (-) of 100 μg/ml Dox for five days were transiently transfected with pEGFP or pEGFP-T17NRac1. The next day, the transfected cells were seeded on NIH3T3 monolayers and incubated for 17 hours. Cells were stained for CADM1 (blue). Scale bar, 10 μm.

Figure 4. CADM1 and Tiam1 are colocalized at the leading edge of ATL-3I cells. ***A.*** Colocalization of CADM1 with Tiam1 at the peripheral margin of ATL-3I cells. Cells were seeded on a monolayer of HMVEC and cultured for 17 hours. Cells were double-stained for CADM1 (green) and Tiam1 (red) with a chicken anti-CADM1 mAb (3E1) and a rabbit anti-Tiam1 pAb (C16), respectively, and then examined by confocal microscopy. Scale bar, 10 μm. A linescan graph of CADM1 (green) and Tiam1 (red) fluorescence intensities is shown. Fluorescence intensities were measured over white dotted line from a to b in the merged panel. Arrows in the graph indicate the position of the cell edges. The patterns of CADM1 and Tiam1 intensities are similar and high at the edges of the cell. ***B.*** A dominant negative mutant of Rac1, T17NRac1, blocked CADM1-induced lamellipodia formation. ATL-3I cells transfected with pEGFP or pEGFP-T17NRac1 were cocultured on a HMVEC monolayer for 17 hours and stained for CADM1 (blue) and actin (red). Scale bar, 10 μm. ***C.*** CADM1 colocalized with the leading edge marker Talin, but not with the trailing edge marker CD44 at the invasive front of ATL3I cells. Panels ***a-f*** show X-Z sections of ATL3I cells adhered to NHDF. CADM1 was colocalized with Talin (***a-c***), but not with CD44 (***d-f***) at the invasive front of ATL3I cells. ATL-3I cells co-cultured on a NHDF monolayer for 6 hours were double-stained for CADM1 (green) and Talin (red, in panels ***b*** and ***c***) or CD44 (red in panels e and f) with 3E1 and a mouse anti-Talin mAb or mouse anti-CD44 mAb (C26), respectively. Note that intense staining of

CADM1, not CD44, is seen at the adhesion sites of ATL-3I cells to NHDF. Illustrations of the cells are depicted above the top panels (***a, d***) with red arrows that indicate direction of cell migration. Scale bar, 10 μm. ***D.*** CADM1 and Tiam1 colocalized at the invasive front of ATL3I cells. Panels ***a-h*** show X-Z sections of ATL cells attached to the NHDF monolayer. Cells were triple-stained for CADM1 (green), Tiam1 (red) and CD44 (blue) with 3E1, C16 and C26, respectively. White arrows show colocalization of CADM1 and Tiam1 at the ventral surface of ATL-3I cells invading the NHDF monolayer (***a-d***) and at the leading edge of ATL-3I cells adhering to the monolayer (***e-h***). Illustrations of the cells are depicted above the top panels (***a, e***) with red arrows that indicate direction of cell migration. Scale bars, 5 μm.

Figure 5. Both CADM1 and Tiam1 are required for lamellipodia formation in HTLV-1 transformed cell lines and ATL cell lines. ***A.*** siRNA-mediated CADM1 and Tiam1 knockdown. Control siRNA (cont), CADM1-specific siRNA (CADM1#1 and CADM1#2) or Tiam1-specific siRNA (Tiam1#1 and Tiam1#2) was introduced into C91/PL cells with electroporation. Forty-eight hours after electroporation, lysates were prepared and 5 μg of the lysates were analyzed by immunoblot with anti-CADM1 pAb (CC2) and anti-Tiam1 pAb (C16). Signals of α-tubulin are shown as loading controls in the bottom panel. Red and blue arrows indicate Tiam1 and CADM1, respectively. ***B.*** CADM1 knockdown disrupted cell aggregates of MT-4 cells. Phase-contrast images were taken 48 hours after introduction of siRNA CADM1 by electroporation. Note that although similar results were obtained in C91/PL cells and ATL-3I cells, disruption of cell aggregates by CADM1 knockdown was most prominent in MT-4 cells. Original magnification, 100x. ***C.*** CADM1 knockdown reduced cell growth of C91/PL, MT-4 and ATL-3I cells. Seven days after electroporation, living cells were counted by trypan blue dye exclusion. Each bar represents the mean $\pm$ SD of triplicate assays. The asterisks indicate statistical significance with $p<0.05$ as determined by the Student's *t* test. ***D.*** Either CADM1 or Tiam1 knockdown impaired cell adhesion to NHDF monolayers. Forty-eight hours after electroporation, Calcein AM-labeled cells were cocultured on NHDF monolayers for two hours. Each bar represents the mean $\pm$ SD of three independent experiments. The asterisks indicate statistical significance with $p<0.05$ as determined by the Student's *t* test. ***E.*** Either CADM1 or Tiam1 knockdown abrogated lamellipodia formation of C91/PL cells cultured on a NHDF monolayer. C91/PL cells treated with specified siRNA were co-cultured on NHDF monolayers for 6 hours. Cells were double-stained for CADM1 (green) and Tiam1 (red) with a chicken anti-CADM1 mAb (3E1) and a rabbit anti-Tiam1 pAb (C16), respectively. Scale bars, 10 μm. Note that either CADM1 knockdown or Tiam1 knockdown not only inhibits lamellipodia formation, but also affects the membrane localization of Tiam1 or CADM1.

Figure 6. Colocalization of CADM1 and Tiam1 in lymph node lesions of ATL patients. ***A.*** Immunohistochemical staining for CADM1 and Tiam1. Tissues were incubated with a rabbit anti-CADM1 pAb (#6) (left panels) or a rabbit anti-Tiam1 pAb (C16) (right panels) and stained with aminoethylcarbazole. The nuclei were counterstained with hematoxylin. Representative images of the CADM1+/Tiam1+ specimens are shown. Original magnification, 200x (upper panels) and 400x (bottom panels). ***B.*** Colocalization of CADM1 and Tiam1 at the cell membrane of infiltrating ATL cells. Immunofluorescence double-staining of sections for CADM1 (green) and Tiam1 (red) was performed with a chicken anti-CADM1 mAb (3E1) and a rabbit anti-Tiam1 pAb (C16). Scale bars, 50 μm.

Figure 7. A possible role of CADM1 in ATL cells. CADM1 comprises three Ig loops modified with N-linked and O-linked glycosylation, a single membrane-spanning α-helix and a short cytoplasmic domain. The cytoplasmic domain has a protein 4.1-BM connected to the actin cytoskeleton through members of the protein 4.1 family and a type II PDZ-BM interacting with Tiam1. CADM1, therefore, seems to recruit actin and a regulator of actin, RacGEF, together to the juxtamembrane region leading to Rac activation for actin reorganization. Domains of Tiam1 abbreviated are described in the legend to Fig. 1*B*.

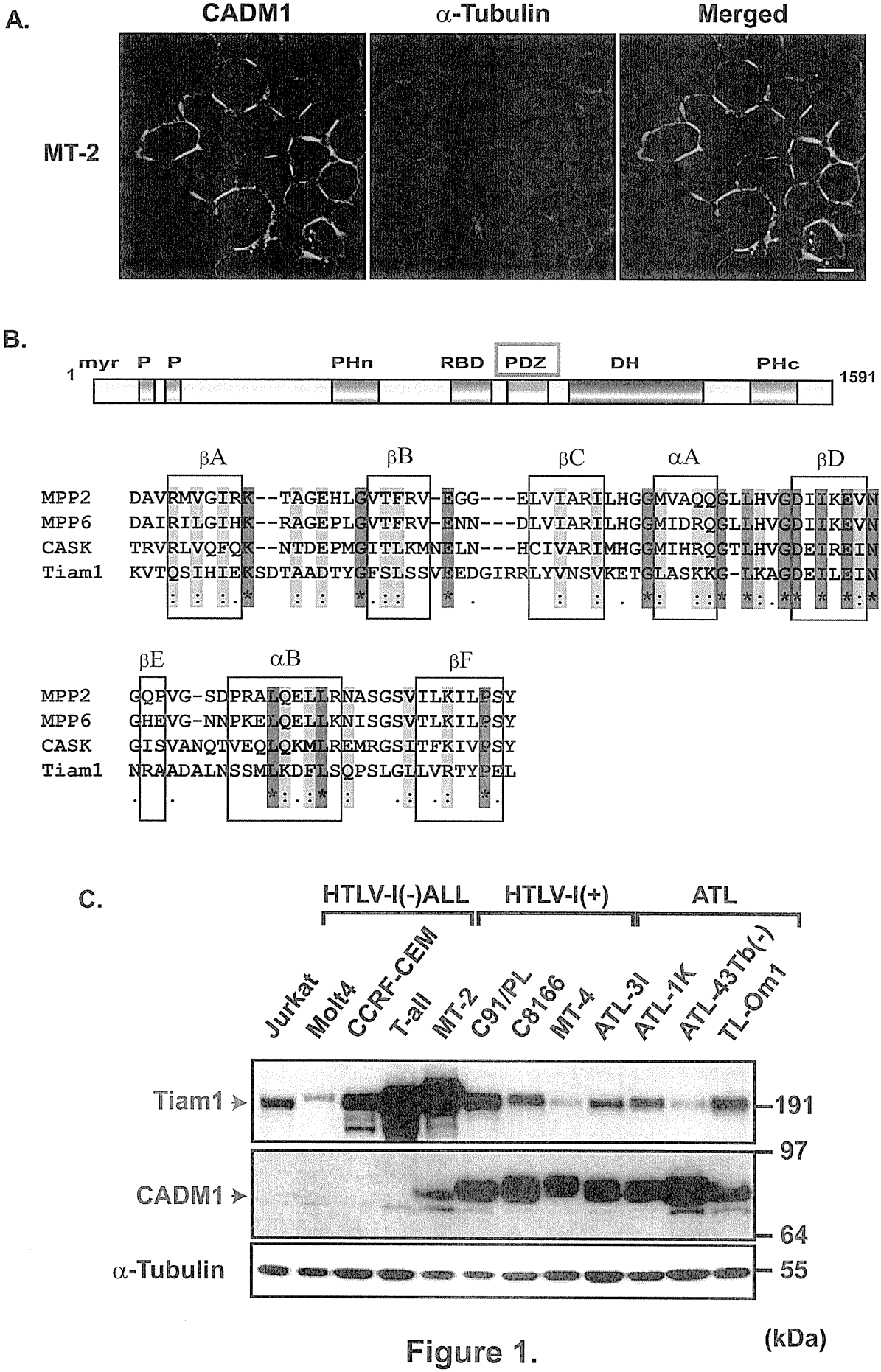
A.
CADM1
α-Tubulin
Merged
MT-2
B.
1
myr
P
P
PHn
RBD
PDZ
DH
PHc
1591
βA
βB
βC
αA
βD
MPP2 DAVRMVGIRK--TAGEHLGVTFRV-EGG---ELVIARILHGGMVAQQGLLHVGDIIKEVN
MPP6 DAIRILGIHK--RAGEPLGVTFRV-ENN---DLVIARILHGGMIDRQGLLHVGDIIKEVN
CASK TRVRLVQFQK--NTDEPMGITLKMNELN---HCIVARIMHGGMIHRQGTLHVGDEIREIN
Tiam1 KVTQSIHIEKSDTAADTYGFSLSSVEEDGIRRLYVNSVKETGLASKKG-LKAGDEILEIN
βE
αB
βF
MPP2 GQPVG-SDPRALQELLRNASGSVILKILPSY
MPP6 GHEVG-NNPKELQELLKNISGSVTLKILPSY
CASK GISVANQTVEQLQKMLREMRGSITFKIVPSY
Tiam1 NRAADALNSSMLKDFLSQPSLGLLVRTYPEL
C.
HTLV-I(-)ALL
HTLV-I(+)
ATL
Jurkat
Molt4
CCRF-CEM
T-all
MT-2
C91/PL
C8166
MT-4
ATL-3I
ATL-1K
ATL-43Tb(-)
TL-Om1
Tiam1
CADM1
α-Tubulin
191
97
64
55
(kDa)

Figure 1.

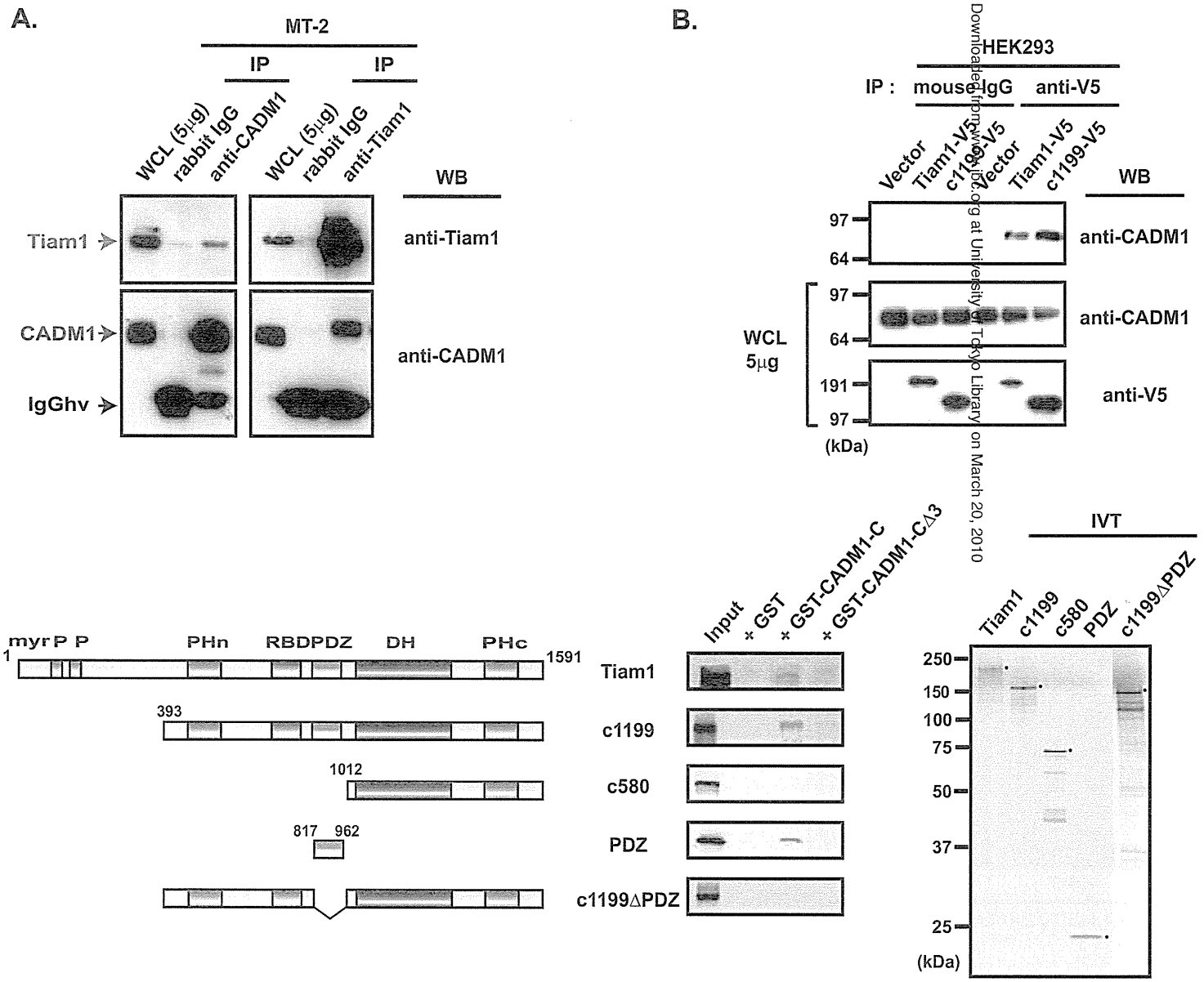

Figure 2.